BASIC SCIENCE

Nanomedicine: Nanotechnology, Biology, and Medicine
13 (2017) 853–861

Original Article

nanomedjournal.com

High-throughput bioaccumulation, biotransformation, and production of silver and selenium nanoparticles using genetically engineered *Pichia pastoris*

Fatemeh Elahian, PhD[a], Somayeh Reiisi, PhD[b], Arman Shahidi, MSc[c], Seyed Abbas Mirzaei, PhD[a,*]

[a]*Cellular and Molecular Research Center, Shahrekord University of Medical Sciences, Shahrekord, Iran*
[b]*Department of Genetics, Faculty of Basic Sciences, University of Shahrekord, Shahrekord, Iran*
[c]*Department of Medical Biotechnology, School of Medicine, Zanjan University of Medical Sciences, Iran*

Received 23 December 2015; accepted 17 October 2016

Abstract

A genetically modified *Pichia pastoris* strain overexpressing a metal-resistant variant of cytochrome b5 reductase enzyme was developed for silver and selenium biosorption and for nanoparticle production. The maximum recombinant enzyme expression level was approximately 31 IU/ml in the intercellular fluid after 24 h of incubation, and the capacity of the recombinant biomass for the biosorption of silver and selenium in aqueous batch models were measured as 163.90 and 63.71 mg/g, respectively. The ions were reduced in the presence of enzyme, leading to the formation of stable 70–180 nm metal nanoparticles. Various instrumental analyses confirmed the well-dispersed and crystalline nature of the spherical nanometals. The purified silver and selenium nanoparticles exhibited at least 10-fold less cytotoxicity toward HDF, EPG85–257, and T47D cells than silver nitrate and selenium dioxide. These results revealed that the engineered *Pichia* strain is an eco-friendly, rapid, high-throughput, and versatile reduction system for nanometal production.

Key words: Biosorption; Cytochrome b5 reductase; Heavy metals; Nanoparticle; Recombinant yeast

Nanoparticles are defined as particles that are approximately between 1 and 100 nanometers in size. Recently, the importance of nanoparticles and nanomaterials has increased due to their unique physicochemical properties and their wide applicability in numerous fields, mainly electronics, chemistry, energy conservation, biosensors, and pioneer medicine.[1] Commercial electrochemical methods are widely used for the production of metal nanoparticles but can be unwieldy, water-inefficient, require the use of large amounts of energy, and generate unwanted hazardous substances; higher levels of initial investment are required to accrue sufficient return.[2] However, the environmentally conscious synthesis of nanoparticles based on the use of microorganisms is obtaining favorable attention due to its simplicity, cost-effectiveness, environmental safety, eco-friendliness, robustness and high-speed, facile, room-temperature production.[3,4]

Metal nanoparticles are mainly biosynthesized in bacteria, actinomycetes, fungi, yeasts, and plants.[5] Fungi and yeasts are best choice for the synthesis of metallic nanoparticles based on silver, gold, cadmium, palladium, and selenium because they secrete enzymes and are easy to manipulate and culture on simple media. Moreover, even in the presence of large amounts of metal ions, these microorganisms can survive and proliferate due to their ability to resist metal stress.[6,7] Chemical ecology is the scientific study of the interactions and relationships between living organisms and their microenvironment. Species that developed the enzymatic capacity to detoxify metal pollution in their habitat survived while others became extinct. The

Funding sources: The authors are grateful for financial support from the Zanjan University of Medical Sciences (grant numbers: A-12-543-5 and A-12-543-7) and Shahrekord University of Medical Sciences (grant number: 1393-01-74-2373).

Conflict of interest: We certify that there is no financial conflict of interest involving any organization.

*Corresponding author at: Cellular and Molecular Research Center, Shahrekord University of Medical Sciences, Shahrekord, Iran.

E-mail addresses: mirzaei.a@skums.ac.ir, dr_amirzaei@yahoo.com, mirzaei@zums.ac.ir (S.A. Mirzaei).

http://dx.doi.org/10.1016/j.nano.2016.10.009
1549-9634/

mechanisms conferring these capacities include the overexpression of efflux pumps; metal precipitation and eliminating metal toxicity using oxidoreduction enzyme cascades; the bioaccumulation of toxic molecules in particular compartments; and the lack of special transporters.[8–10]

Silver and Selenium have historically been important due to their broad-spectrum applications in chemistry, computers, cosmetics, electronics, industrial dyes, and textile manufacturing[11,12] and are among the essential trace supplements that act as successful antimicrobial, antifungal and antibiofilm agents, interact with proteins to inhibit cellular damage, control thyroid function, modulate immune surveillance, inhibit tumor cell invasion and angiogenesis, promote differentiation, and regulate cell proliferation and death.[13–15] Regardless of these benefits, window of therapeutic concentration of Ag and Se ions is narrow; for this reason, studies are now focusing on how to overcome the disadvantages of high doses of silver and selenium using their nanoparticle counterparts.[16,17]

Silver and selenium nanoparticle biosynthesis by microorganisms and plant cells has been described in several studies.[18] In addition to low-throughput intact cell strategies for nanomaterial biosynthesis, other methods involving the use of cell extracts, cell-free supernatants, and pure enzymes have also been employed.[19,20] Although pure oxidoreductive enzymes have been reported to catalyze high-quality and efficient metal biotransformation, several laborious and costly enzyme purification, stabilization and immobilization processes are required. Furthermore, these enzymes cannot function alone, but require coenzymes. Preferential oxidoreductive coenzymes, such as NADH and NADPH are expensive and are seldom economically feasible for use with current enzyme technologies.[21]

To the best of our knowledge, we report for the first time the intracellular biosynthesis of stable, less toxic and highly dispersed silver and selenium nanoparticles using genetically modified *Pichia pastoris* overexpressing *Mucor racemosus* cytochrome b5 reductase enzyme (Cyb5R). We previously isolated and characterized this filamentous fungus from polluted industrial effluents and sewage water; specific attention was paid to the Cyb5R enzyme due to its high resistance to heavy metals.[21,22] Cloning this enzyme enabled *Pichia* to grow in the presence of toxic ions through the intracellular reduction and sequestration of nanometals and led to the cost-efficient high-throughput biosorption and biotransformation of metals. The engineered yeast synthesizes the required coenzymes and cofactors in an eco-friendly manner. Such protocols would revolutionize the mining industries, nanometal bioproduction, and the biological remediation of environmental pollution.

Methods

Cells, reagents and media

Silver nitrate ($AgNO_3$) and selenium dioxide (SeO_2) were purchased from Sigma–Aldrich (St. Louis, USA). RPMI-1640 medium, trypsin, fetal bovine serum (FBS), penicillin and streptomycin were obtained from Gibco (Grand Island, NY, USA). Vectors, Zeocin, X-33 host strains, positive expression controls, *Pichia* transformation reagents, and media components for yeast culture were obtained from Invitrogen (NY, USA). All other chemicals and solvents were of analytical grade and were purchased from Merck (Darmstadt, Germany).

Codon optimization of soluble Cyb5R and Pichiacloning

Previously, the genome of *Mucor racemosus* and *Pichia pastoris* were studied, and the levels of codon usage were determined. The gene for the soluble isoform of *Mucor* NADH-cytochrome b5 reductase (*GI: 167,614,335*) was codon-optimized for expression in *P. Pastoris* and then synthesized. The gene encoding 228 amino acids was sub-cloned in pPICZB between *Xho*I and *Xba*I for intracellular tag-free recombinant protein production. Transformation was performed according to Invitrogen's instructions. Briefly, after the corresponding plasmid pPICZB-Cyb5R was linearized using *Sac*I within the 5′ AOX1 region, the X-33 strain was chemically transformed. All putative multiple copy recombinants were assayed for the Mut^+ or Mut^S phenotypes using AOX1 primers. Intracellular enzyme activity was measured using the NADH-dependent ferricyanide reduction method; one unit of Cyb5R activity was defined as the amount of enzyme required to reduce 1 μmol ferricyanide in 1 min.[22]

Metal ion resistance and growth kinetics

The X33 parental strain and several stable and Mut^+ recombinant counterpart clones were cultivated for 24 h in 500-ml Erlenmeyer flasks containing 100 ml of YPD broth (1% w/v yeast extract, 2% w/v peptone, 2% w/v glucose). Subsequently, the cells were subcultured in fresh media containing 0.5% methanol (which was used to activate the AOX1 promoter and express the recombinant enzyme) to reach an initial OD600 of approximately 0.01; $AgNO_3$ and SeO_2 stock solutions were then added separately to the cell suspension to yield final concentrations of 0, 1, 2, 4, 6, 8, 10, 20, and 40 mM. The flasks were incubated for 96 h on an orbital shaker at 30 °C and were sampled four times daily. The maximum specific growth rate (μ_{max}) was estimated for all cultures according to the linear least square method based on the natural logarithms of the optical density values at 600 nm (measured at the beginning of the exponential phases) and several time points. The slope of the best fitted line was considered to represent μ_{max}.

Nanoparticle production kinetics

For the biosynthesis of Ag and Se nanoparticles (NPs), a fresh culture of engineered *Pichia pastoris* was passaged in 500-ml conical flasks containing 100 ml of YPD and 0.5% methanol. The cultures were then cultivated overnight to an OD600 of approximately 1. Filter-sterile stock solutions of $AgNO_3$ or SeO_2 were added to the cell mixture at final concentrations of 6 mM and 4 mM, respectively. Negative controls were grown on heavy metal-free YPD medium. The biomass was sampled twice daily for 96 h and freeze dried separately. Subsamples (0.5 g) were digested using microwave-assisted acid digestion according to EPA 3052 for biological samples. Briefly, 9 ml of concentrated nitric acid, 1 ml of fuming HCl, and 2 ml of H_2O_2 were added to samples in PTEF vessels. The reagents were allowed to react for approximately 1 minute before sealing the vessels. The tubes

Table 1
Maximum specific growth rate of biomass treated with various ion concentrations according to a mathematical model.

	0 mM	1 mM	2 mM	4 mM	6 mM	8 mM	10 mM	20 mM	40 mM
Transformed yeast treated with Ag	$\mu = 0.53^a$ $R^2 = 0.96$	$\mu = 0.42^b$ $R^2 = 0.91$	$\mu = 0.41^b$ $R^2 = 0.93$	$\mu = 0.39^b$ $R^2 = 0.90$	$\mu = 0.40^b$ $R^2 = 0.90$	$\mu = 0.25^c$ $R^2 = 0.85$	$\mu = 0.21^c$ $R^2 = 0.81$	$\mu = 0.11^c$ $R^2 = 0.73$	GI
Non-transformed yeast treated with Ag	$\mu = 0.51^a$ $R^2 = 0.97$	$\mu = 0.44^b$ $R^2 = 0.96$	$\mu = 0.12^c$ $R^2 = 0.76$	GI	GI	GI	GI	GI	GI
Transformed yeast treated with Se	$\mu = 0.53^a$ $R^2 = 0.96$	$\mu = 0.41^b$ $R^2 = 0.95$	$\mu = 0.40^b$ $R^2 = 0.94$	$\mu = 0.41^b$ $R^2 = 0.95$	$\mu = 0.35^c$ $R^2 = 0.96$	$\mu = 0.13^d$ $R^2 = 0.97$	$\mu = 0.12^d$ $R^2 = 0.81$	$\mu = 0.12^d$ $R^2 = 0.86$	GI
Non-transformed yeast treated with Se	$\mu = 0.51^a$ $R^2 = 0.97$	$\mu = 0.33^b$ $R^2 = 0.87$	GI	GI	GI	GI	GI	GI	GI

μ: maximum specific growth rate average during the early exponential growth phase (1/h).
R^2 (R-squared): a regression coefficient that indicates how well the data fits the statistical model.
GI: growth inhibition and the onset of yeast sporulation. No statistical model was fitted, or the R-squared value was less than 0.7.
Values in the same row marked with the same letters are not significantly different ($P > 0.05$) according to the homogeneity of variance obtained using ANOVA analysis.

were then placed in a microwave oven (Multiwave 3000™, PerkinElmer, USA) and heated to 180 °C for at least 15 minutes. After cooling, the metal contents were quantified by analyzing Ag and Se in the TX-114-rich phase using ICP-OES (Optima, USA) according the manufacturer's protocol.

Purification of nanoparticles

A fresh overnight culture of recombinant *Pichia* was treated with 6 mM $AgNO_3$ or 4 mM SeO_2 and incubated for 3 days. Cells were then harvested by centrifugation at 5000×*g* for 10 min. The pellet was washed twice with 0.8% w/v NaCl in 100 mM phosphate buffer. The cells were then resuspended in fungal lysis buffer (0.5% v/v Triton ×100; 1% w/v SDS; 100 mM NaCl; 1 mM EDTA; 10 mM Tris pH = 8) and homogenized using SilentCrusher™ (Heidolph, Germany). The suspension was centrifuged at 14,000×*g* for at least 15 minutes. The resulting pellet containing metal nanoparticles was washed twice with 1.5 M Tris/HCl buffer (pH 8.3) containing 1% SDS and then resuspended in distilled water. The nanoparticles were purified three times using a two-phase, water/octanol extraction system. Pure nanometal sediments at the tube bottom were washed with chloroform, ethyl alcohol, and distilled water, in that order, and then freeze-dried.[23]

X-ray diffraction identity and particle size analyses

A small amount of the pure nanoparticles was resuspended in distilled water and homogenized using ultrasonication (75 watts) for 2 min. The particle size distribution and charge potential were evaluated using dynamic light scattering and a zeta size analyzer (ZEN3600, Malvern, UK). X-ray diffraction spectra of pure Ag and Se powders were recorded at the wide-angle range of 2θ from 10 to 80 degrees at increments of 0.02-degree using a powder X-ray diffractometer (STOE, Germany).

Electron microscopy and atomic force microscopy

TEM measurements were recorded using an EM10C TEM system (EM10C-100KV, Zeiss, Germany) operating at a voltage of 120 keV. The samples were prepared on carbon-coated copper TEM grids by drop-coating with suspensions of homogenized Ag and Se. The suspension cell or pure colloidal nanoparticles were smeared on a glass slide for high-resolution images using scanning electron microscope (FESEM, Zeiss, Germany) at an accelerating voltage of 15.0 kV. For atomic force microscopy (AFM), 10 μL of Ag and Se nanoparticle colloidal suspensions were spread onto the surface of a dust-free cover slips, dried at room temperature, and mounted on AFM (JPK, Deutschland) stubs. The size of the Ag and Se nanoparticles was evaluated, and the thickness was measured using the package particle analysis function in the software according to standard protocols.

Human cell culture and cytotoxicity assay

Primary human dermal fibroblasts (HDF; NCBI Number Index: C646) were purchased from cell lines service (Pasteur, Iran). EPG85–257 (human gastric carcinoma) and T47D (human epithelial breast cancer) cell lines were generously provided by Professor Herman Lage (Molecular Pathology Department, University of Medicine Berlin, Germany). The cells were cultured in RPMI medium containing 2 mM L-glutamine, 10% (v/v) FBS, 100 IU/ml penicillin, and 100 mg/ml streptomycin at a constant temperature of 37 °C in a humidified CO_2 incubator. Cells were seeded into 96-well tissue culture plates (1000 cells per well) containing various concentrations of metal ions (0–1000 μM) or nanoparticles (0–10,000 μM) for 5 days. Afterward, the cells were treated with MTT (5 mg/ml) at 37 °C for 3 h. Formazan crystals were measured using a TECAN microplate reader at 570 nm. IC_{50} values were defined as the drug concentration that reduced the surviving fraction of cells in each well by 50% compared to the untreated cells.[24,25]

Statistical analysis

All experiments were performed at least three times independently, and the results are expressed as the mean values ± SE. The data were compared using Student's t-test. P-values of less than 0.01 were considered statistically significant.

Results

Cloning and evaluation of metal ion resistance

The gene coding for the full-length enzyme including a sequence recognized by the restriction endonucleases *Xba*I and *Xho*I was synthesized. Cloning, transformation, and verification of the clones were performed in *E. coli* strain DH5α and then the

Figure 1. Color changes in bioreduction batches using engineered *Pichia*. After 0 h (left), after 24 h of exposure to 6 mM $AgNO_3$ (middle), and after 24 h of exposure to 4 mM SeO_2 (right).

right recombinant structure subcloned in X33-*Pichia pastoris*. Maximal total enzyme activity was measured as 31 IU/ml in the intercellular fluid after 24 h of incubation using 0.5% methanol for expression induction. The growth kinetics for the parent and engineered yeast were monitored in the presence and absence of various concentrations of $AgNO_3$ and SeO_2 in the range from 0 to 40 mM (Table 1). Wild-type parental yeast strains did not resist ion concentrations of greater than 1 mM. Although the transformants were resistant to metal ions even at concentrations of 10 mM, the maximum specific growth rate and nanoparticle production were markedly decreased. The highest ion concentrations that did not reduce the maximum specific growth rate significantly ($P > 0.05$) were 6 mM of $AgNO_3$ (corresponding to 647.2 μg/ml of elemental silver) and 4 mM of SeO_2 (corresponding to 315.8 μg/ml of elemental selenium).

Nanoparticle production kinetics

The results obtained confirmed that recombinant *Pichia pastoris* efficiently reduced $AgNO_3$ and SeO_2 to uncharged metal nanoparticles. The color of the medium changed due to the generation of nanoparticles (from initial light orange to metallic gray and red for Ag and Se production, respectively) after 24 h of incubation (Figure 1). The maximum retention capacities were approximately 163.90 and 63.71 mg/g for silver and selenium, respectively (Figure 2). Silver and selenium production kinetics followed a natural logarithmic curve that was expressed as $Y = 12.05 \times Ln(t) + 106.04$ and $Y = 4.38 \times Ln(t) + 40.96$ with squared regression coefficients of 0.93 and 0.94, respectively (where Y denotes milligrams of nanometal per gram of dried yeast weight and t is the time in hours). Yeast growth kinetics were fitted to the following natural logarithmic equations: $Ln(X) = 0.40 \times t - 4.34$ and $Ln(X) = 0.41 \times t - 4.20$ for growth in 6 mM $AgNO_3$ and 4 mM SeO_2, respectively, with squared regression coefficients of 0.90 and 0.95, respectively, during the early exponential growth phase; in the equations, X represents biomass, and t is the time elapsed in hours (Supplementary Figure 1 and Table 1). Metal biosorption apparently occurs during the trophophasic phase of recombinant yeast growth,

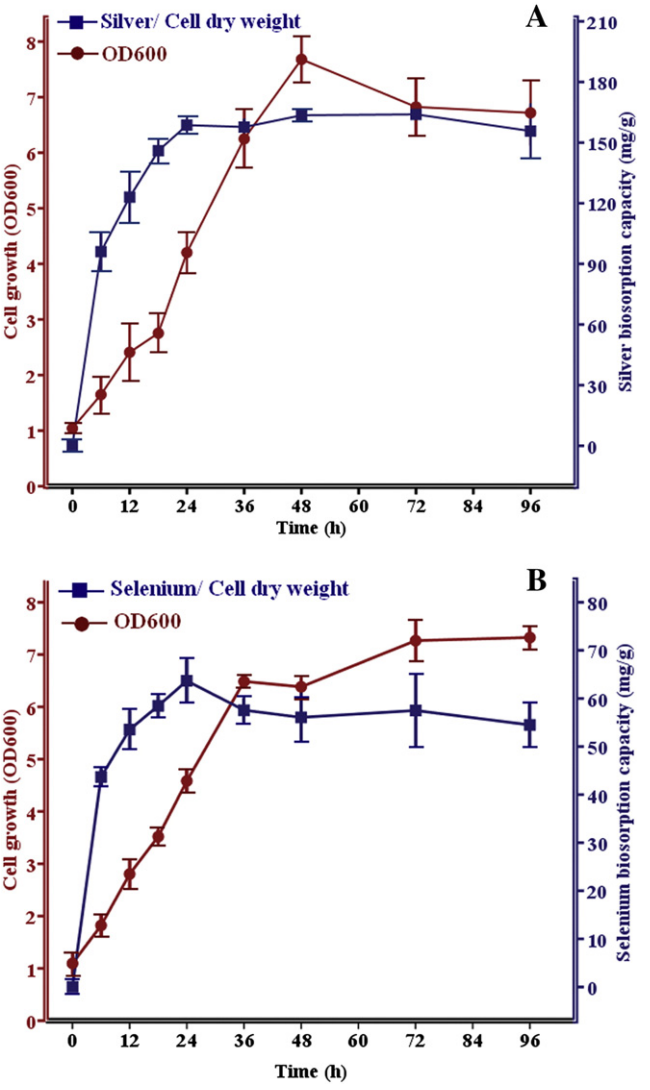

Figure 2. Recombinant yeast growth and nanoparticle production. Recombinant yeasts were treated with 6 mM silver nitrate (**A**) or 4 mM selenium dioxide (**B**). Fresh samples were collected twice daily and subsequently analyzed. Cell growth was monitored based on absorbance at 600 nm and dry cell weight. Intracellular nanometal production was measured instrumentally using ICP-OES. The values represent the means of three independent experiments (mean ± standard error).

coinciding with the production of recombinant Cyb5R. Biosorption yield (%) is calculated by dividing the actual intracellular nanometal mass to the theoretical elemental mass added at time zero (Table 2); Percent yield is used to measure biosorption reaction efficiency under certain conditions.

Identification and characterization of nanoparticles

X-ray diffraction spectra were obtained to determine the crystalline nature and identity of the Ag and Se nanoparticles (Figure 3). The XRD-spectra showed four sharp extreme peaks in the total spectrum of 2θ values from 10 to 80; this result reflects the crystalline structure of pure Ag and Se. Figure 4 shows AFM and TEM micrographs of the purified nanoparticles.

Table 2
Percent yield of metal biosorption against time.

Time (h)	0	6	12	18	24	36	48	72	96
Silver biosorption yield (%)[a]	0.00 ± 0.00	17.92 ± 2.11	23.42 ± 3.66	38.63 ± 2.31	65.78 ± 2.74	73.19 ± 1.38	76.04 ± 1.90	81.06 ± 1.94	84.12 ± 3.14
Selenium biosorption yield (%)	0.00 ± 0.00	0.50 ± 3.86	41.44 ± 2.77	50.00 ± 2.06	63.38 ± 3.22	64.17 ± 3.12	67.79 ± 3.78	73.14 ± 3.01	72.82 ± 2.65

The data represent the mean ± standard error of three individual experiments.
[a] Silver nitrate and selenium dioxide were present at 6 mM and 4 mM, respectively, in the cell reactors and biosorption yields were calculated by dividing actual yields by theoretical yields.

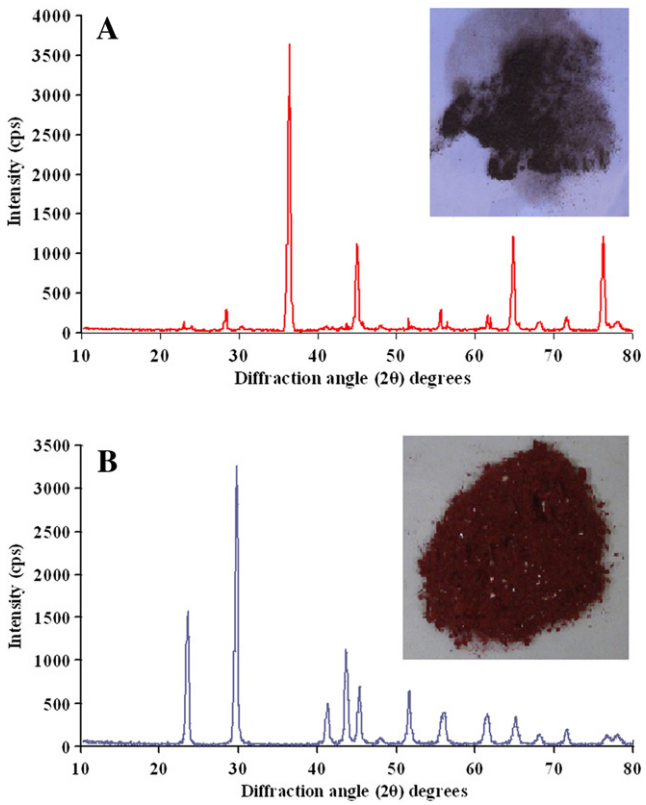

Figure 3. X-ray diffractogram of silver (A) and selenium (B) nanoparticles. Diffraction patterns confirmed the presence of nano-sized elemental silver and selenium as the major constituents. Sharp intensive peaks indicate small crystalline particle size.

The Ag and Se NPs were spherical and ranged from 70 to 180 nm in diameter. The particle sizes of the Ag and Se particles were assessed using TEM and AFM and were very similar (to the crystallite size predicted using the particle size analyzer (Supplementary Figure 2).

Cytotoxicity Assay

The HDF, EPG85–257 and T47D cell lines were treated with increasing doses of selenium dioxide, sliver nitrate, nanosilver, and nanoselenium. A dose–response curve was fitted to the resulting data, and the IC_{50} values were calculated after 5 days of exposure in MTT cell viability assays (Figure 5). The cells were also treated with mitoxantrone as a positive control for cell cytotoxicity. The most cytotoxic effect was exerted by $AgNO_3$ on the HDF line ($P < 0.001$; IC_{50} value, approximately 0.25 μM). In contrast, nanoselenium appeared to have the least toxicity on the T47D line ($IC_{50} > 5$ mM elemental selenium). The obtained data showed that the cytotoxic effects of these compounds are dose-dependent and cell-specific (Table 3).

Discussion

Many chemical reactors are available commercially and are designed empirically to synthesize nanoparticles in the colloidal and aerosol phases. Unfortunately, the large-scale, economic, and eco-friendly synthesis of monodispersed nanoparticles remains challenging.[26,27] Recently, improved biological technologies have attracted attention to the synthesis and application of metallic nanoparticles. Microorganisms (bacteria, yeasts and fungi) can interact with particular ions and reduce them to metal nanoparticles. In this regard *Pichia pastoris* proves to be a safe and important biological reactor for intracellular biosynthesis of stable nanoparticles. This yeast is much more resistant to metal toxicity, grows rapidly in inexpensive simple media, produces high yields of biomass and is easily manipulated genetically. Here a simple and element-specific reduction of metal ions catalyzed enzymatically by NADH dependent cytochrome b5 reductase. The bioproduction of silver and selenium nanoparticles can be visually followed by the medium color changes to metallic gray and red, respectively, during the early hours of ions exposure (Figure 1). These colors arise from excitation of surface plasmon resonances in the nanometals.[28]

Previously native nitrate reductase, cytochrome c reductase, and cytochrome P450 reductase have been noticed for mild metal bioremediation. However, traditional enzyme technology costs remained high because in nature, organisms adjust the conditions of their enzymes to produce an optimum rate of reaction, it is technically very difficult to recover and immobilize active enzymes, and much of the cost relates to cofactor supplementation.[19,20,29] On the hand overexpressing a metal-resistant variant of cytochrome b5 reductase in our study resulted in *Pichia* resistance to high concentrations of heavy metal ions rather than native microorganisms and provided high yields of nanometals.

Based on literature review the magnitude of silver and selenium uptake capacity by native yeasts can be estimated as 2–50 mg/g and 0.016–1.58 mg/g, respectively. In contrast, silver accumulates in our engineered *Pichia* at 163.90 mg/g and selenium is biosorbed at 63.71 mg/g; these levels (Figure 2)

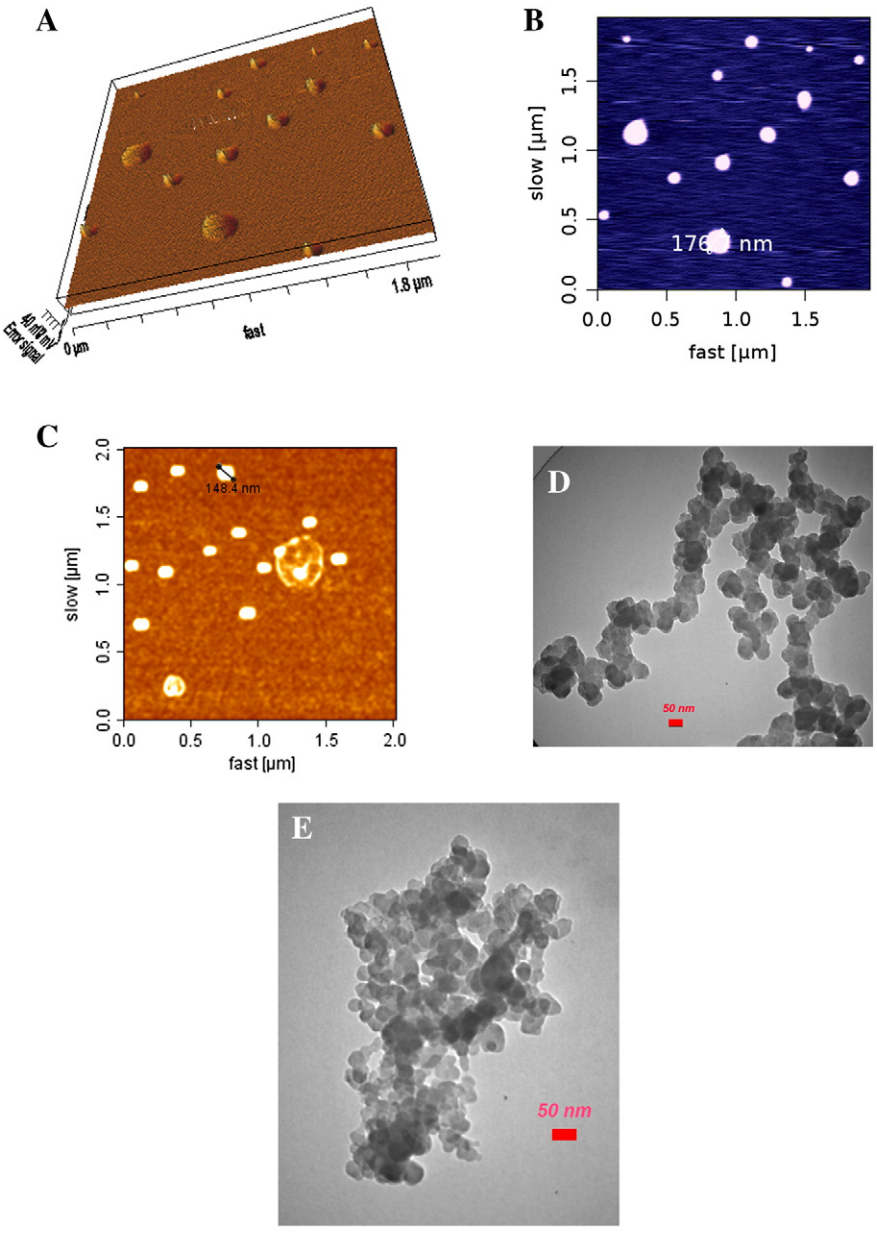

Figure 4. Examples of metal biotransformation using recombinant *Pichia*. (**A**, **B**) AFM image of silver nanometals. (**C**) AFM image of pure selenium nanometals. (**D**, **E**) TEM image of silver and selenium nanometals. Microscopic analyses revealed the predominately spherical shape of the intracellular nanoparticles (average diameter, 70 to 180 nm).

represent the highest levels of these metals biosorption that have been reported.[30–32] The levels of bioaccumulation of silver and selenium that were measured in this study are similar to those measured in wild-type plants; however, yeast biomass apparently accumulates more easily and more rapidly.[33,34]

Although the recombinant cells resisted metallic ion concentrations approximately 20-fold higher than those that the parental cells could withstand, the cell growth kinetics was affected. Cellular decrease in maximum specific growth rate (Table 1) in presence of silver and selenium ions might have been due to the general toxicity of the ions toward the metabolic pathways and is considered the main disadvantage of growing cell biotransformations.[23,35] Other reasons that might cause low biomass yield in the presence of high ion levels in this overexpression/biocatalysis approach are the inhibition of yeast cell respiration and the high consumption of NADH and O_2 in the enzyme-based bioremediation technique.[36]

Figure 4 and Supplementary Figure 2 micrographs revealed that the most of silver and selenium nanoparticles were uniformly spherical and were in the range of 70–180 nm in size; hence, it could be understood that the nanometals exhibited well-defined dimensions and good monodispersity and the experimental conditions such as metal ion concentrations, media compositions, fermentation conditions, and cofactor availability were almost optimum. Particle size and monodispersity were controlled more easily using this novel approach

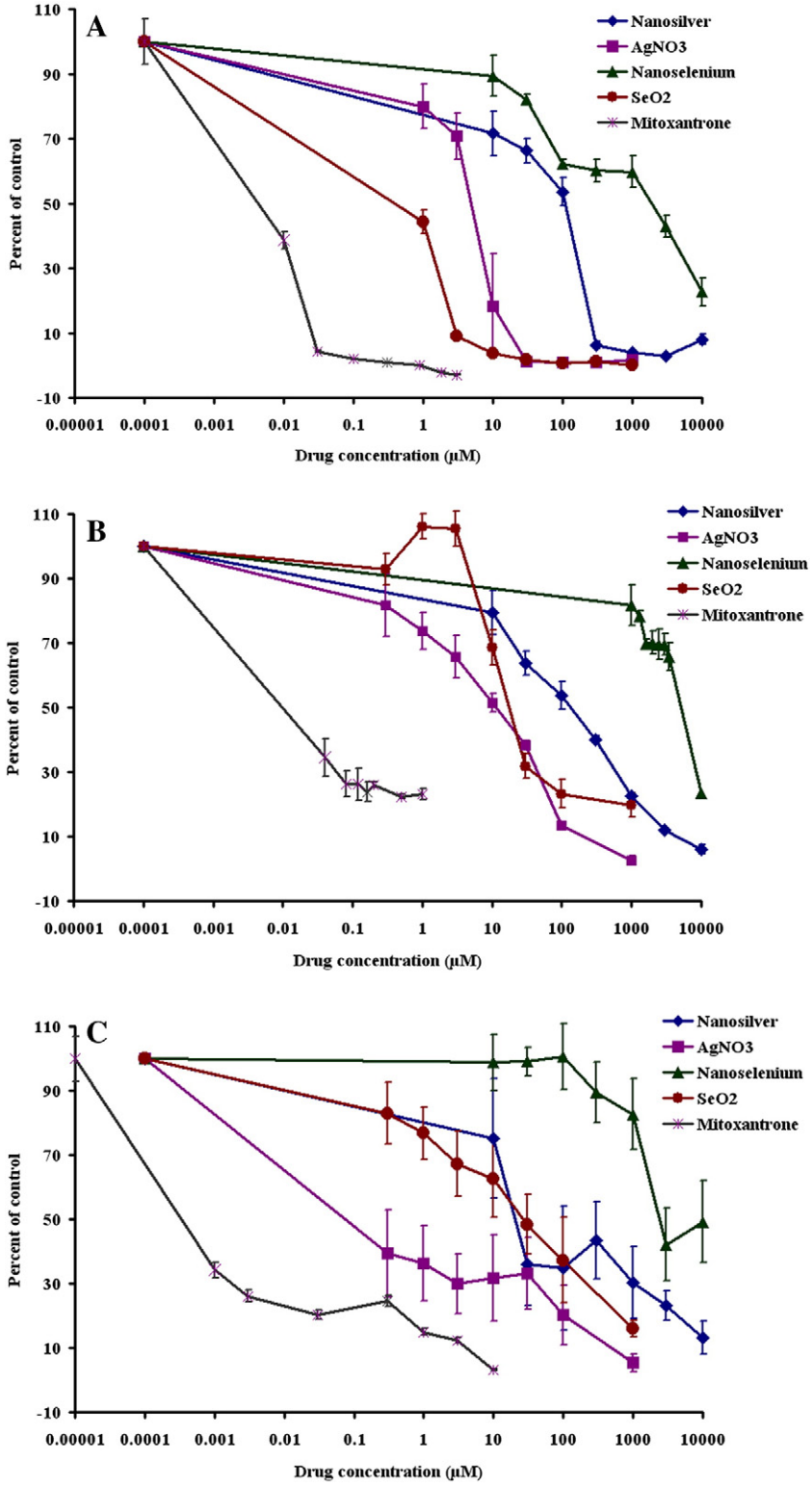

Figure 5. Effects of selenium dioxide, silver nitrate, nanosilver, or nanoselenium on cell survival in EPG85–257 (**A**), T47D (**B**), and HDF (**C**). The cells were cultured for 5 days with increasing doses of the compounds from 0 to 10,000 μM. Cell survival was measured using the MTT assay. The values represent the means of three independent experiments, which were performed in triplicate (mean ± SE).

than by using chemical methods or non-recombinant yeasts and wild-type bacteria.[37–39] In the literature, silver and selenium particle sizes ranged from 5 to 200 nm; such differences in the size of nanoparticles produced by biological methods are common. Normally fast and strong reducing enzymes and biomolecules are used to produce smaller nanoparticles.

Table 3
IC50 values of mitoxantrone, nanometals and their corresponding ions for the primary dermal fibroblasts and cancer cell lines.

Cells	$AgNO_3$ IC_{50}[a] ± SE	Nanosilver IC_{50} ± SE	Mitoxantrone IC_{50} ± SE	SeO_2 IC_{50} ± SE	Nanoselenium IC_{50} ± SE
EPG85–257	5.77 ± 0.414***	115.29 ± 6.097***	0.01 ± 0.004	0.85 ± 0.521***	2152.49 ± 49.818***
T47D	12.32 ± 0.721***	153.71 ± 10.107***	0.03 ± 0.004	20.06 ± 1.613***	5927.14 ± 50.203***
HDF	0.25 ± 0.137***	22.81 ± 4.831***	0.0007 ± 0.000	27.74 ± 4.012***	2612.07 ± 113.328***

The data represent the mean ± standard error of three individual experiments.
[a] The drug concentration (μM) required for 50% inhibition of cell growth after 5 days of drug exposure.
*** Indicates statistical significance between the nanometal and its ion counterpart ($P < 0.001$).

Physicochemical production of nanoparticles is often performed in the presence of stabilizers in order to control of the nuclei formation and prevent unwanted agglomeration of the colloids; such methods involving chemical agents are associated with environmental toxicity and more difficult to be optimized.[40,41] Low average values of Zeta potential (data not shown) are mainly caused by the high tendency of nanometals to aggregate in aqueous intracellular environments. Human albumin was successfully used to reduce elemental aggregation in this study. A comparison of the measured IC_{50} values in Table 3 revealed that nano-sized insoluble particles were at least 10-fold less toxic toward HDF, EPG85–257, and T47D cell lines rather than their soluble $AgNO_3$ and SeO_2. Normal HDF cells were more sensitive to the metal toxicity than cancerous T47D cells. Different responses in the activity of the key enzymes in metal metabolism are the most possible explanation for differential cytotoxicity in these cells. The cytotoxicity of the nanoparticles and their ion counterparts showed a direct dose-dependence and cell viability was reduced at higher concentrations consistent with many reports.

The results obtained here show that silver and selenium nanoparticles were successfully biosynthesized using an engineered metal-resistant *Pichia pastoris* clone containing Cyb5R. The biosynthesis of nanoparticles using the engineered yeast represents a potential alternative to conventional biological and traditional physicochemical methods; the advantages include high throughput, the production of less toxic waste, cost-effectiveness, simplicity, reduced time requirements, eco-friendliness, and the production of homogenous nanometals.

Author Contributions

S.A. Mirzaei coordinated the study, designed the cloning and biotransformation experiments, and revised the final manuscript. F. Elahian designed the cytotoxicity study and performed the statistical analysis, wrote the corresponding portions of the manuscript, and participated in intellectual discussions of the data and manuscript writing. S. Reiisi engineered the *Pichia* clones and analyzed the enzyme activity. A. Shahidi performed most of the experiments as part of his master's degree in medical biotechnology.

Appendix A. Supplementary data

Supplementary data to this article can be found online at http://dx.doi.org/10.1016/j.nano.2016.10.009.

References

1. Daniel MC, Astruc D. Gold nanoparticles: assembly, supramolecular chemistry, quantum-size-related properties, and applications toward biology, catalysis, and nanotechnology. *Chem Rev* 2004;**104**:293-346.
2. Dhillon GS, Brar SK, Kaur S, Verma M. Green approach for nanoparticle biosynthesis by fungi: current trends and applications. *Crit Rev Biotechnol* 2012;**32**:49-73.
3. Bansal V, Rautaray D, Bharde A, Ahire K, Sanyal A, Ahmad A, et al. Fungus-mediated biosynthesis of silica and titania particles. *J Mater Chem* 2005;**15**:2583-9.
4. Azad AK, Amin L, Sidik NM. Genetically engineered organisms for bioremediation of pollutants in contaminated sites. *Chin Sci Bull* 2014;**59**:703-14.
5. Singh P, Kim YJ, Zhang D, Yang DC. Biological synthesis of nanoparticles from plants and microorganisms. *Trends Biotechnol* 2016;**34**:588-99.
6. Sastry M, Ahmad A, Islam Khan M, Kumar R. Biosynthesis of metal nanoparticles using fungi and actinomycete. *Curr Sci* 2003;**85**:162-70.
7. Balaji DS, Basavaraja S, Deshpande R, Mahesh DB, Prabhakar BK, Venkataraman A. Extracellular biosynthesis of functionalized silver nanoparticles by strains of Cladosporium cladosporioides fungus. *Biointerfaces* 2009;**68**:88-92.
8. Bhainsa KC, D'Souza SF. Extracellular biosynthesis of silver nanoparticles using the fungus aspergillus fumigatus. *Biointerfaces* 2006;**47**:160-4.
9. Bruins MR, Kapil S, Oehme FW. Microbial resistance to metals in the environment. *Ecotoxicol Environ Saf* 2000;**45**:198-207.
10. Iravani S. Green synthesis of metal nanoparticles using plants. *Green Chem* 2011;**13**:2638-50.
11. Lara HH, Garza-Trevino EN, Ixtepan-Turrent L, Singh DK. Silver nanoparticles are broad-spectrum bactericidal and virucidal compounds. *J Nanobiotechnol* 2011;**9**:30.
12. Tran PA, Webster TJ. Selenium nanoparticles inhibit *Staphylococcus aureus* growth. *Nanomedicine* 2011;**6**:1553-8.
13. Zeng H, Combs GF. Selenium as an anticancer nutrient: roles in cell proliferation and tumor cell invasion. *J Nutr Biochem* 2008;**19**:1-7.
14. Zhang R, Lee P, Lui VC, Chen Y, Liu X, Lok CN, et al. Silver nanoparticles promote osteogenesis of mesenchymal stem cells and improve bone fracture healing in osteogenesis mechanism mouse model. *Nanomedicine* 2015;**11**:1949-59.
15. Fu X, Yang Y, Li X, Lai H, Huang Y, He L, et al. RGD peptide-conjugated selenium nanoparticles: antiangiogenesis by suppressing VEGF-VEGFR2-ERK/AKT pathway. *Nanomedicine* 2016;**12**:1627-39.
16. Ramamurthy C, Sampath KS, Arunkumar P, Kumar MS, Sujatha V, Premkumar K, et al. Green synthesis and characterization of selenium nanoparticles and its augmented cytotoxicity with doxorubicin on cancer cells. *Bioprocess Biosyst Eng* 2013;**36**:1131-9.
17. Tutaj K, Szlazak R, Szalapata K, Starzyk J, Luchowski R, Grudzinski W, et al. Amphotericin B-silver hybrid nanoparticles: synthesis, properties and antifungal activity. *Nanomedicine* 2016;**12**:1095-103.
18. Shikuo L, Yuhua S, Anjian X, Xuerong Y, Xiuzhen Z, Liangbao Y, et al. Rapid, room-temperature synthesis of amorphous selenium/protein composites using *Capsicum annuum* L extract. *Nanotechnology* 2007;**18**:405101.

19. Anil Kumar S, Abyaneh MK, Gosavi SW, Kulkarni SK, Pasricha R, Ahmad A, et al. Nitrate reductase-mediated synthesis of silver nanoparticles from AgNO3. *Biotechnol Lett* 2007;**29**:439-45.
20. Mukherjee P, Senapati S, Mandal D, Ahmad A, Khan MI, Kumar R, et al. Extracellular synthesis of gold nanoparticles by the fungus fusarium oxysporum. *Chem Bio Chem* 2002;**3**:461-3.
21. Elahian F, Sepehrizadeh Z, Moghimi B, Mirzaei SA. Human cytochrome b5 reductase: structure, function, and potential applications. *Crit Rev Biotechnol* 2014;**34**:134-43.
22. Mirzaei SA, Yazdi MT. Sepehrizadeh Z secretory expression and purification of a soluble NADH cytochrome b5 reductase enzyme from Mucor Racemosus in Pichia Pastoris based on codon usage adaptation. *Biotechnol Lett* 2010;**32**:1705-11.
23. Shakibaie M, Khorramizadeh MR, Faramarzi MA, Sabzevari O, Shahverdi AR. Biosynthesis and recovery of selenium nanoparticles and the effects on matrix metalloproteinase-2 expression. *Biotechnol Appl Biochem* 2010;**56**:7-15.
24. Mansouri M, Mirzaei SA, Lage H, Mousavi SS, Elahian F. The cell cycle arrest and the anti-invasive effects of nitrogen-containing bisphosphonates are not mediated by DBF4 in breast cancer cells. *Biochimie* 2014;**99**:71-6.
25. Elahian F, Moghimi B, Dinmohammadi F, Ghamghami M, Hamidi M, Mirzaei SA. The anticancer agent prodigiosin is not a multidrug resistance protein substrate. *DNA Cell Biol* 2013;**32**:90-7.
26. Roco MC. Nanoparticles and nanotechnology research. *J Nanopart Res* 1999;**1**:1-6.
27. Turner M, Golovko VB, Vaughan OP, Abdulkin P, Berenguer-Murcia A, Tikhov MS, et al. Selective oxidation with dioxygen by gold nanoparticle catalysts derived from 55-atom clusters. *Nature* 2008;**454**:981-3.
28. Dar MA, Ingle A, Rai M. Enhanced antimicrobial activity of silver nanoparticles synthesized by Cryphonectria sp evaluated singly and in combination with antibiotics. *Nanomedicine* 2013;**9**:105-10.
29. Macdonald IDG, Smith WE. Orientation of cytochrome c adsorbed on a citrate-reduced silver colloid surface. *Langmuir* 1996;**12**:706-13.
30. Donmez G, Aksu Z. The effect of copper(II) ions on the growth and bioaccumulation properties of some yeasts. *Process Biochem* 1999;**35**:135-42.
31. Kapoor A, Viraraghavan T. Fungal biosorption - an alternative treatment option for heavy metal bearing wastewaters: a review. *Bioresour Technol* 1995;**53**:195-206.
32. Wang J, Chen C. Biosorption of heavy metals by *Saccharomyces cerevisiae*: a review. *Biotechnol Adv* 2006;**24**:427-51.
33. Nettem K, Almusallam AS. Equilibrium, kinetic, and thermodynamic studies on the biosorption of selenium (IV) ions onto Ganoderma Lucidum biomass. *Separ Sci Technol* 2013;**48**:2293-301.
34. Wang J, Chen C. Biosorbents for heavy metals removal and their future. *Biotechnol Adv* 2009;**27**:195-226.
35. Quijano G, Couvert A, Amrane A, Darracq G, Couriol C, Le Cloirec P, et al. Toxicity and biodegradability of ionic liquids: new perspectives towards whole-cell biotechnological applications. *Chem Eng J* 2011;**174**:27-32.
36. Allen C, Boudet C, Hardacre C, Migaud M. Enhancement of whole cell dioxygenase biotransformations of haloarenes by toxic ionic liquids. *RSC Adv* 2014;**4**:19916-24.
37. Mohanpuria P, Rana NK, Yadav SK. Biosynthesis of nanoparticles: technological concepts and future applications. *J Nanopart Res* 2008;**10**:507-17.
38. Levard C, Hotze EM, Lowry GV, Brown GE. Environmental transformations of silver nanoparticles: impact on stability and toxicity. *Environ Sci Technol* 2012;**46**:6900-14.
39. Valls M, Atrian S, de Lorenzo V, Fernández LA. Engineering a mouse metallothionein on the cell surface of *Ralstonia eutropha* CH34 for immobilization of heavy metals in soil. *Nat Biotechnol* 2000;**18**:661-5.
40. Sharma G, Sharma AR, Bhavesh R, Park J, Ganbold B, Nam JS, et al. Biomolecule-mediated synthesis of selenium nanoparticles using dried *Vitis vinifera* (raisin) extract. *Molecules* 2014;**19**:2761-70.
41. Sharma VK, Yngard RA, Lin Y. Silver nanoparticles: green synthesis and their antimicrobial activities. *Adv Colloid Interface Sci* 2009;**145**:83-96.